Taylor & Francis
Taylor & Francis Group

Canadian Water Resources Journal / Revue canadienne des ressources hydriques

ISSN: 0701-1784 (Print) 1918-1817 (Online) Journal homepage: http://www.tandfonline.com/loi/tcwr20

Modelling Climate Change Impacts on Spring Runoff for the Rocky Mountains of Montana and Alberta II: Runoff Change Projections using Future Scenarios

Robert P. Larson , James M. Byrne , Dan L. Johnson , Stefan W. Kienzie & Matthew G. Letts

To cite this article: Robert P. Larson , James M. Byrne , Dan L. Johnson , Stefan W. Kienzie & Matthew G. Letts (2011) Modelling Climate Change Impacts on Spring Runoff for the Rocky Mountains of Montana and Alberta II: Runoff Change Projections using Future Scenarios , Canadian Water Resources Journal / Revue canadienne des ressources hydriques, 36:1, 35-52, DOI: 10.4296/cwrj3601035

To link to this article: http://dx.doi.org/10.4296/cwrj3601035

Published online: 23 Jan 2013.

Modelling Climate Change Impacts on Spring Runoff for the Rocky Mountains of Montana and Alberta II: Runoff Change Projections using Future Scenarios

Robert P. Larson, James M. Byrne, Dan L. Johnson, Stefan W. Kienzle, and Matthew G. Letts

Abstract: In Part I of this two-part study, the Simulated Grid microclimate model (SIMGRID) was modified and the new version validated on the St. Mary River watershed in northern Montana, using historical data. In Part II, future climate change scenarios are used to estimate spring streamflow (Q_S) for the 1961-2099 period. Relative to the base period (1961-1990), the model indicates median year Q_S decline of 3 - 8% by the 2020s, 8 - 17% by the 2050s, and 15 - 27% by the 2080s. Mean onset of the spring pulse is projected to occur in early March or late February for the 2080s, 36 to 50 days earlier than for the 1961-1990 reference period. Model results generally indicate increased precipitation, but spring runoff volumes will decrease substantially, because the higher rain:snow ratio and shorter accumulation period will decrease snowpack volume. Overall, the results of this study indicate that the increased winter temperature resulting from anthropogenically-induced climate change, will result in shorter winters, reduced snowpack volume, and earlier spring snowmelt and runoff onset, resulting in substantial reductions in spring discharge.

Résumé: Dans la Partie I de la présente étude en deux parties, le modèle de microclimats alpin « SIMGRID » a été modifié et la nouvelle version a été validée sur le bassin versant de la rivière St. Mary dans le nord du Montana, en utilisant des données historiques. Dans la Partie II, les scénarios de changements climatiques futurs ont été utilisés pour estimer l'écoulement fluvial au printemps (Q_S) pour la période de 1961 à 2099. Par rapport à la période de base (1961-1990), le modèle indique une diminution de la médiane de Q_S de 3 à 8 % d'ici les années 2020, de 8 à 17 % d'ici les années 2050 et de 15 à 27 % d'ici les années 2080. En moyenne, le début de l'écoulement de printemps est prévu pour fin février ou début mars au cours des années 2080, c'est-à-dire de 36 à 50 jours plus tôt que pendant la période de référence (1961-1990). Malgré une prévision d'augmentation des précipitations, les modèles indiquent également une diminution considérable du volume d'écoulement printanier causé par une hausse du ratio pluie/neige et par la diminution de la période d'accumulation entrainant la diminution du volume du manteau

Robert P. Larson, James M. Byrne, Dan L. Johnson, Stefan W. Kienzle, and Matthew G. Letts

Department of Geography, Water and Environmental Science Program, University of Lethbridge, 4401 University Dr., Lethbridge, AB, Canada, T1K 5A7

Submitted January 2010; accepted October 2010. Written comments on this paper wil be accepted until September 2011.

de neige. De manière générale, les résultats de cette étude indiquent que l'augmentation des températures hivernales découlant du changement climatique anthropique se traduira par des hivers plus courts, une réduction du volume du manteau de neige et une fonte prématurée du manteau de neige, entraînant ainsi une réduction substantielle des écoulements printaniers.

Introduction

Climate warming presents a considerable threat to industrial, municipal, environmental and recreational stakeholders, in regions where water supply is derived from snow-dominant headwaters (Barnett *et al.*, 2005). Western North America (WNA) surface air temperatures have risen at an overall mean rate of 0.1 – 0.2˚C per decade since 1950, with more pronounced warming observed during the winter and spring seasons (Karl *et al.*, 1993; Lettenmaier *et al.*, 1994; Mote *et al.*, 2005; Vincent *et al.*, 1999). As a result, widespread snowpack declines (Brown and Braaten, 1998; Hamlet *et al.*, 2005; Mote, 2003; Mote *et al.*, 2005; Selkowitz *et al.*, 2002), higher rain:snow ratios (Knowles *et al.*, 2006), shorter snow accumulation seasons, and more frequent winter melt periods (Hamlet *et al.*, 2005; Nash and Gleick, 1991; Shabbar and Bonsal, 2003) have been observed. Each of these changes can result in decreased streamflow volume and changes to runoff quantity and timing.

Previous historical summaries indicated that the date of peak snowmelt is occurring approximately 1 - 4 weeks earlier compared to the last half century (Groisman *et al.*, 1994; Stewart *et al.*, 2005). Annual flows for many Rocky Mountain regions has declined by 0.22 % y^{-1} over the last century (Rood *et al.*, 2005a). Seasonal trends indicate that winter flows are increasing, and that summer and early autumn flows are decreasing. The largest seasonal declines are in late summer flows (-0.2 % y^{-1}), which have occurred for the rivers draining the eastern slopes of the Rocky Mountains (Rood *et al.*, 2008).

Global circulation model (GCM) outputs suggest temperature increases of 2 to 6˚C in WNA by 2100 (Field *et al.*, 2007) and modest increases in annual precipitation. Seasonal precipitation may decrease in some regions and/or show much greater variation (Christensen *et al.*, 2007). Declines in snowpack volume are, thus, expected to continue in response to warming. For example, volumes are expected to decline by 60 - 100% in US coastal regions (e.g., Cascade mountains) and in the US southwest (e.g., Sierra Nevada mountains) by the end of the century (Leung *et al.*, 2004; Leung and Wigmosta, 1999; McCabe and Wolock, 1999). Warmer winter temperatures may also accelerate spring snowmelt and the onset of the spring streamflow pulse. Stewart *et al.* (2004; 2005) estimated that peak flows would occur 30-40 days earlier in the future, relative to the observed 1948-2000 trends.

Hydrologic response at the watershed scale is less certain, mainly because of differing precipitation regimes. A wetter and warmer climate could shift watershed streamflow to a more rainfall-dominated regime (Whitfield *et al.*, 2002), especially in areas west of the continental divide (Loukas *et al.*, 2002; 2004; Morrison *et al.*, 2002). For example, the Okanagan watershed could experience increases in runoff especially in the near-term. However, it is likely that temperature increases will overwhelm precipitation increases, resulting in runoff decline over the long-term (Merritt *et al.*, 2006). East of the continental divide, few studies have considered the potential impact of climate warming on the hydrology of montane watersheds. This may be due, in part, to contradictions in the magnitude and direction of projected snowpack volume changes. Differences between studies arise from the distinct modelling approaches used. For example, McCabe and Wolock (1999) reported 9% and 3% increases in snowpack volume for the 2025-2034 and 2090-2099 periods, for the Montana-Alberta Rocky Mountain region, based on analysis of GCM outputs. Leung and Wigmosta (1999), on the other hand, used GCM output to drive a Regional Climate Model (RCM), which captured orographic effects. They predicted an 18% snowpack volume decrease in a representative watershed of the Montana-Alberta Rocky Mountain region within the next century.

Lapp *et al.* (2002; 2005) downscaled GCM data for use in a high resolution mountain snow accumulation and ablation model and projected a 38% reduction in snowpack volume for a mountain watershed (1445 km^2 area) in the southern Alberta Rockies by 2020-2050. Increasing precipitation is a source of potential snow water equivalent (SWE), but increasing temperature outweighed this effect, so that SWE was projected to decline. Therefore, watershed-scale assessments are needed to determine the net effect of these influences

over complex terrain, and to more accurately simulate associated hydrologic changes.

Study Rationale

The St. Mary headwaters study basin is located on the eastern slopes of the Rocky Mountains in Glacier National Park, Montana. It is the principal water source for almost 200,000 ha of downstream irrigation in southern Alberta (Canada) and 56,600 ha in Montana (United States) (Alberta Agriculture, Food & Rural Development (AAFRD), 2000). The river water supply in these semi-arid regions is fully allocated in most years. Multiple on- and off-stream water storage facilities, in conjunction with interbasin diversion systems, have facilitated extensive irrigation developments. However, these developments have resulted in major ecosystem impacts (Rood *et al.*, 1995; Rood *et al.*, 2005b) and conflict with regard to transboundary water allocation (Halliday and Faveri, 2007). Intensive livestock operations, irrigation-based crop production and rapid urban growth also impact water quality and quantity in the region (Byrne *et al.*, 2006; Schindler and Donahue, 2006).

In the last two decades, St. Mary River water users have suffered through supply shortfalls in 1988 and 2001. During the 2001 drought, water rationing measures were implemented according to St. Mary River (SMR) Project recommendations. Reduced discharge was due to a series of circumstances, including shallow winter snowpack, spring soil moisture depletion from a lack of precipitation, and maintenance-related low reservoir levels (R. Renwick, SMR Irrigation District, pers. comm.). Repeated maintenance-related supply problems are unlikely to occur, but the frequency of low SWE and soil moisture depletion are expected to increase in response to climate warming.

The objective of this paper is to model spring streamflow volume and timing for the St. Mary River watershed during the 21st century, based on a range of climate warming scenarios. The model used was developed and calibrated using historical data in Part I of this two-part study (Larson *et al.*, this issue). Part II of this study is an exercise that aims to provide a first estimate of hydrologic changes in response to climate change using a set of GCM outputs. Two assumptions are necessary for this type of research. Firstly, GCM scenarios are presumed to accurately portray the future. Secondly, we must assume that the characteristics of the hydrologic system will remain as they are depicted in the model. A detailed description of the study area and modelling approach is found in Larson *et al.* (this issue).

To accomplish the objective, climate change scenarios derived from the results of six global circulation models (GCMs), were selected for three future periods (2020s, 2050s, and 2080s). Using the climate record for the 1961-1990 base period, we then used the "delta method" to produce the downscaled climate scenarios for the St. Mary basin. Finally, the modified version of the Simulated Grid microclimate (SIMGRID) Snow-Runoff model, validated for the 1961-1990 climate record (Larson *et al.*, this issue), was applied.

Materials and Methods

SIMGRID Snow-Runoff Model

The SIMGRID model (Shepperd, 1996, Lapp, 2005) was refined and applied to the simulation of snow water equivalent (SWE) and spring streamflow volume. Details of the model development may be found in Larson *et al.* (this issue). The SIMGRID Snow-Runoff model is driven by daily precipitation and temperature. The model comprises the Mountain Microclimate Simulation (MTCLIM) Model (Hungerford *et al.*, 1989), which extrapolates base weather station data to outlying mountain sites of varying aspect, slope, and elevation.

The SIMGRID Snow-Runoff model spatially extrapolates the base weather station data to the extent of a watershed, which is defined by terrain categories (TC). Terrain categories represent areas of equal terrain attribute combinations, and are derived from a digital elevation model (DEM) of the study area.

The model simulates snow accumulation and melt, including rain-on-snow, for all TCs. Total potential snowmelt runoff (S_R) and rainfall runoff (R_R) volumes are compiled. The variable S_R refers to the total amount of meltwater that is available for runoff or infiltration. The variable R_R refers to the amount of precipitation that occurs on assumed saturated soils that is available for runoff or infiltration.

The SIMGRID Snow-Runoff model was run for the 1961-1990 calibration years. From the output, S_R was determined for the period between the mean watershed

Julian date of maximum snow accumulation (*Jmax*) and the final Julian date of snowpack disappearance (*Jdis*); R_R was determined for the period following *Jdis*. *Jmax* and *Jdis* vary across the watershed and depend on the hydrometeorology of the TCs.

For each year, the S_R and R_R output were summed for the watershed, and expressed as million m^3. Finally, the S_R and R_R independent variables were regressed against observed spring streamflow volume (Q_s) for each year. Thus using physically-based variables, a multiple linear regression model was developed to predict runoff.

Scenarios Data

Projected monthly mean minimum and maximum temperature and precipitation data were downloaded for the study region, from the Pacific Climate Impacts Consortium (PCIC) (2007). The values represent the average changes expected for three future time periods (2010-2039, 2040-2059 and 2070-2099), relative to the base period (1961-1990). While the data are said to represent a 30-year period, PCIC only provided GCM output corresponding to one set of monthly changes to be applied for the entire 30-year period (e.g., there were 12 change values for each parameter for the 2020s time slice, which corresponded to the expected monthly changes over the 2010-2039 time period).

We considered 26 climate change scenarios, derived from six GCMs. For each scenario, outputs from the four grid cells surrounding the St. Mary study area were averaged. The grid cells differed slightly for each GCM, in terms of location and size (Table 1). The coarse resolution of GCMs did not capture mountain topography, and the aim was to obtain more representative change values for the study area (Bonsal *et al.*, 2003; Von Storch *et al.*, 1993). The climate change scenarios used in this study included several model runs for each model, including distinct greenhouse gas emission paths. For example, the Canadian Centre for Climate Modelling and Analysis has provided output for the CGCM2 for several runs (e.g., A21, A22, A23, B21, B22, and B23). Output exists for the results of each run corresponding to the 2020s, 2050s, and 2080s. A GCM run is forced by one of many projected greenhouse gas emissions paths, outlined in the Special Report on Emissions Scenarios (Nakićenović *et al.*, 2000) which is distinct for each future time period, and may vary according to the initial model parameters.

Table 1. Study Specific GCM Information. The centre point coordinates of the northwestern cell closest to the St. Mary study area are shown to illustrate the spatial coverage of each model, along with its resolution (defined as the average length of a grid cell side, as well as degrees latitude and longitude). The bolded first letter(s) of the model acronym are those used for labeling the data in Figure 1.

Modelling centre	GCM acronym	NW grid cell centre coordinates	Grid cell resolution
Canadian Centre for Climate for Modelling and Analysis (CCCMA)	**C**GCM2	50.10°N, 116.25°W	339 km; 3.7° lat. x 3.7° long.
Center for climate Research Studies (CCSR) and National Institute for Environmental Studies (NIES), Japan	**CC**SRNIES	52.61°N, 118.12°W	499 km; 5.6° lat. x 5.6° long.
Hadley Centre for climate prediction and Research, England	**H**adCM3	50.00°N, 116.25°W	277 km; 2.5° lat. x 3.75° long.
Commonwealth Scientific and Industrial Research Organization (CSIRO), Australia	**CS**IROMk2b	49.38°N, 118.12°W	386 km; 3.2° lat. x 5.6° long.
National Center for Atmospheric Research (NCAR), United States	**N**CARPCM	48.84°N, 118.12°W	256 km; 2.8° lat. x 2.8° long.
Max Planck Institute for Meteorology, Germany	**E**CHAM4	48.84°N, 118.12°W	256 km; 2.8° lat. x 2.8° long.

Scenario Selection

The Intergovernmental Panel on Climate Change (IPCC) guidelines recommend that more than one scenario be used to capture the range of possible future climate in a particular region (Carter *et al.*, 1999). To develop the climate change scenarios, average projected changes in monthly minimum temperature, maximum temperature and precipitation (ΔT_{min}, ΔT_{max}, and ΔP, relative to 1961-1990), were compiled from the 26 combinations of GCMs and scenarios.

Within each of the three future periods, mean changes in November to June temperature and precipitation varied greatly among the models (Figure 1). This eight-month period was considered exclusively, because the modelling approach validated in Larson *et al.* (this issue) focused on the water balance inputs of winter and spring SWE, as well as spring and early summer rainfall. Barrow and Yu (2005) used a similar method in their scenario selection for an assessment of climate change in the province of Alberta. The uncertainty in model projections in Figure 1 is considerable, and there is a greater degree of scatter observed for later time periods, owing to increased uncertainty (Cubasch *et al.*, 2001). All model scenarios projected increases in mean temperature through the future period, ranging from a minimum of 0.4°C during the 2020s to a maximum of 8.2°C for the 2080s. The cluster of model runs projecting temperature increases of more than 6.0°C for the 2080s were considered as outliers, and were not used in the selection process.

To effectively investigate possible future conditions, two scenarios were selected to be representative of the range of the most common climate change scenarios. When results are extended beyond the single cluster of predictions for the 2020s, two linear clusters were noted, representing high and low precipitation increases (Figure 1). The HadCM3 A1Fl model runs (Scenario 1; upper trend line in Figure 1), were consistent with the high precipitation cluster of climate scenarios. The CCSRNIES B11 model runs (Scenario 2; lower trend line in Figure 1), were characteristic of the low precipitation cluster.

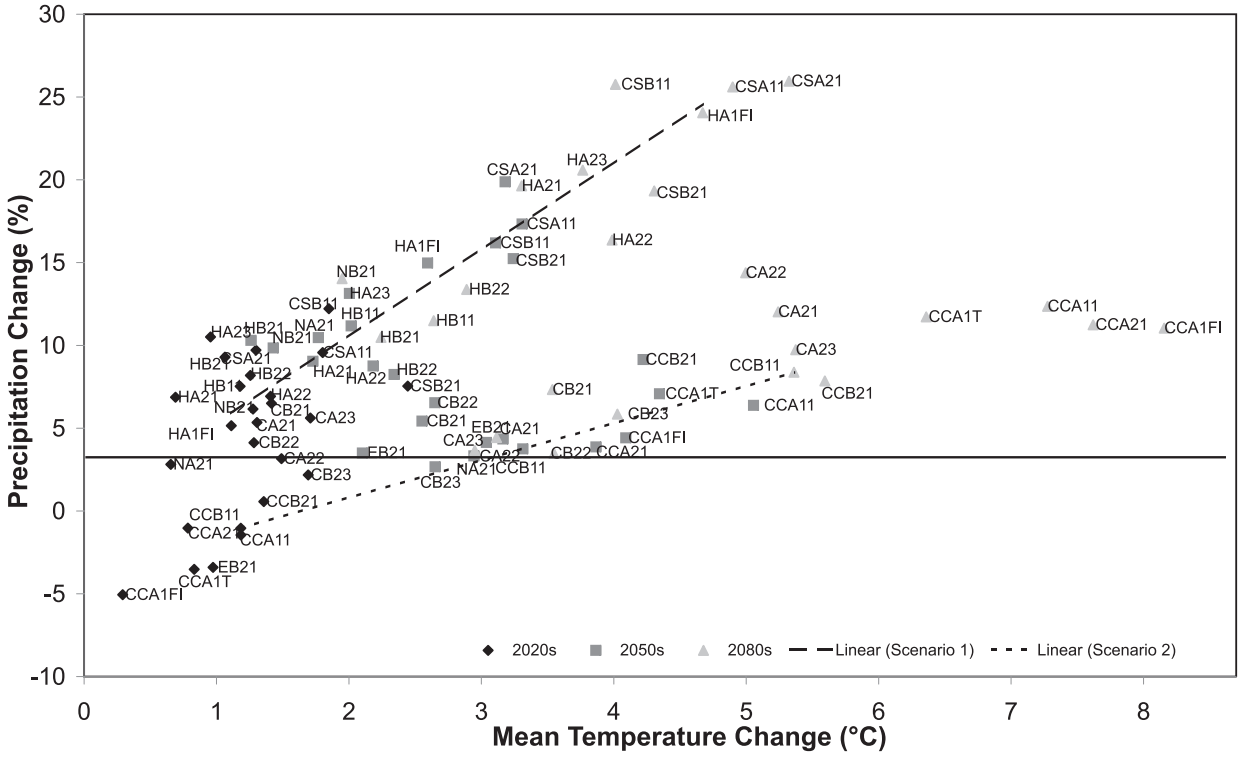

Figure 1. Precipitation and mean temperature changes, relative to 1961-1990, as output from GCM runs for the three future time periods. Results were averaged for the months from November to June. See Table 1 for the abbreviated GCM acronyms, used to label scenarios (along with the emissions scenario identifier and the model experiment number). For example, CB23 denotes the result for the CGCM2 forced by the B2 emissions path, during the 3rd experiment.

Downscaling

Scenarios 1 and 2 were each used to create data sets reflecting annual St. Mary climate change spanning 2010-2099. The monthly ΔT_{max}, ΔT_{min}, and ΔP values for each future period were averaged by season: December through February (DJF), March through May (MAM), June through August (JJA), and September through November (SON). The trend line equations were used to obtain the mean annual change in each variable through the three 30-year periods represented by each time slice (i.e., 2020s, 2050s, and 2080s). Thus ΔT_{max}, ΔT_{min}, and ΔP values were calculated, on a seasonal basis, for a continuous annual time series of incremental change, for each scenario.

The "delta method" was used to apply the changes calculated above to perturb the St. Mary daily climate of the base period (1961-1990). This method has been used in previous climate studies (Loukas *et al.*, 2004; Merritt *et al.*, 2006; Morrison *et al.*, 2002), but it does present limitations. For example, any large-scale patterns of variability present in the base period climate are carried over to the future simulations. However, methods for predicting changes in such phenomena (e.g., Pacific Decadal Oscillation (PDO), Pacific North American Pattern (PNA) and El Niño Southern Oscillation (ENSO), which are linked to external radiative forcing and sea surface temperature distributions, are not well developed (Bond *et al.*, 2003; Hauer *et al.*, 1997; Leung *et al.*, 1999; Newman *et al.*, 2003; Overland and Wang, 2007). Furthermore, negative and positive feedback loops that may be related to such large-scale variability, including cloudiness, snow-albedo and biospheric effects, are not well understood (Betts, 2004; Langen *et al.*, 2007; Qu and Hall, 2007; Sanderson *et al.*, 2005).

The following examples show how the daily temperature and precipitation changes were applied to the St. Mary climate station daily data. The *Tmax* for a future time period, under a future scenario, and for a particular season was (all variables in ˚C):

$$Tmax_i(\mathrm{F}) = Tmax_i(\mathrm{B}) + \Delta Tmax_s(\mathrm{F}) \qquad (1)$$

where $Tmax_i$(F) is the maximum temperature at St. Mary station for the ith day of the future time period, $Tmax_i$(B) is the maximum temperature at St. Mary station for the ith day of the base period daily climate record. $\Delta Tmax_s$(F) is the change in maximum temperature, relative to the base period, for the appropriate season of the ith day for the future time period.

The same method was used to calculate *Tmin*. Future precipitation was obtained by using the percent change to adjust daily historical values, i.e.:

$$P_i(F) = P_i(B) \times (1 + \Delta P_s(F)/100) \qquad (2)$$

where P_i(F) is the future precipitation at St. Mary station for the ith day of the future time period (mm), P_i(B) is the precipitation at St. Mary station, for the ith day of the base period daily climate record (mm), ΔP_s(F) is the change in precipitation, relative to the base period, for the appropriate season of the ith day of the future time period (%).

The variations calculated using climate change scenarios were applied to the 1961-1990 base climate record. The resultant dataset, combining historical 1961-2004 data and modelled 2010-2099 output, covered a 140 year period (with a modest gap from 2005-2009) and reflected graduated warming estimates for Scenarios 1 and 2.

Spring Runoff Model Runs

For each of the three future 30-year period daily climate records, and for each scenario, the following steps were taken to model future changes in snow hydrology:

- The SIMGRID Snow-Runoff model distributed maximum and minimum temperature extremes and precipitation across the study watershed according to 566 terrain categories (TCs) of similar slope, aspect and elevation.
- For each TC, the SIMGRID Snow-Runoff model simulated daily snow accumulation and ablation, with SWE and rainfall outputs.
- Using the modelled data, Julian dates of maximum snowpack accumulation (*Jmax*) and snowpack disappearance (*Jdis*) were determined for the individual TCs, and for the watershed for each year.
- Total potential snowmelt runoff (S_R) and total potential effective rainfall runoff (R_R) volumes for the watershed were compiled from the modelled data, with S_R and R_R volumes computed additively from the contributions

of all the TCs in the watershed (see Larson *et al.*, this issue).

- The statistical spring runoff model, calibrated for the 1961-1990 period and validated in Larson *et al.* (this issue), was applied:

$$Q_S = a + bS_R + cR_R \quad (3)$$

where Q_S is the spring streamflow volume, S_R is the total potential snowmelt runoff volume, R_R is the total potential effective rainfall runoff volume (all units in million m^3), a = -187.15 (SE_a = 54.44; p_a = 0.002), b = 0.682 (SE_b = 0.085; p_b < 0.001), c = 1.004 (SE_c = 0.309; p_c = 0.003), and model R2 = 0.79 (SE = 40.16).

Analysis

Seasonal Climate Changes

Changes in $\Delta Tmax$, $\Delta Tmin$, and ΔP values vary according to the season and the scenario (Table 2). Absolute changes at the St. Mary climate station, shown through seasonal mean temperature (i.e. average of maximum and minimum temperature) and precipitation, relative to the 1961-1990 base period (Figure 2), provide a sense of resultant impacts on snow accumulation and ablation. Snow accumulation generally occurs during the DJF (December, January, and February) season (Figure 2a), while snow ablation begins during the MAM (March, April, May) season (Figure 2b).

During the DJF season, the mean temperature is -4.0°C for the base period. It remains below zero for the 2020s, but passes the critical freezing temperature (solid line in Figure 2a) by the latter period of the 2050s for Scenario 2. Both scenarios indicate above-freezing temperatures for the 2080s for the DJF season. Changes in precipitation are largest for Scenario 1 during the DJF season. For example, Scenario 1 *P* increases from 169 to 240 mm (41.7% increase) during the DJF season from base to 2080s periods, respectively.

For the MAM season, under both scenarios temperatures increase steadily through progressive time periods. The precipitation increase through time is smaller than the precipitation increase during the DJF season. For example, Scenario 1 *P* increases from 208 to 247 mm (18.5% increase) from the base period to the 2080s during the MAM season.

Representative Low, Medium, and High Flow Years

Comparisons of average historical magnitudes to magnitudes under climate warming scenarios provide meaningful long term planning guidance. We also wished to assess how wet and dry (i.e., extreme) flow years may vary under climate change. High, median, and low flow years from the base period frequency distribution were chosen to compare with corresponding future years. This analysis strictly compared changes in magnitude for specific years within the 1961-1990 frequency distribution. The delta method used to downscale the climate change data resulted in the base period frequency distribution merely being shifted to the three future climate change scenario periods. While it is widely accepted that the frequency of temperature and precipitation distributions will change under climate warming (Diffenbaugh *et al.*, 2005; Huntington, 2006), the actual changes in frequency distributions were not analyzed and considered in this study.

Table 2. Seasonal temperature and precipitation changes for each scenario, relative to the 1961-1990 base period. *Tmax* and *Tmin* changes are in °C, and precipitation changes are in %.

Season	Time Period	Scenario 1			Scenario 2		
		$\Delta Tmax$	$\Delta Tmin$	ΔP	$\Delta Tmax$	$\Delta Tmin$	ΔP
DJF	2020s	0.7	1.3	8.3	0.8	0.6	-2.6
	2050s	2.0	3.2	21.3	3.4	3.3	7.3
	2080s	3.5	5.6	41.7	5.6	5.7	10.8
MAM	2020s	0.8	1.1	6.9	1.5	1.7	6.2
	2050s	2.0	2.1	17.5	3.4	3.2	9.9
	2080s	3.9	4.0	18.5	5.3	5.2	15.2

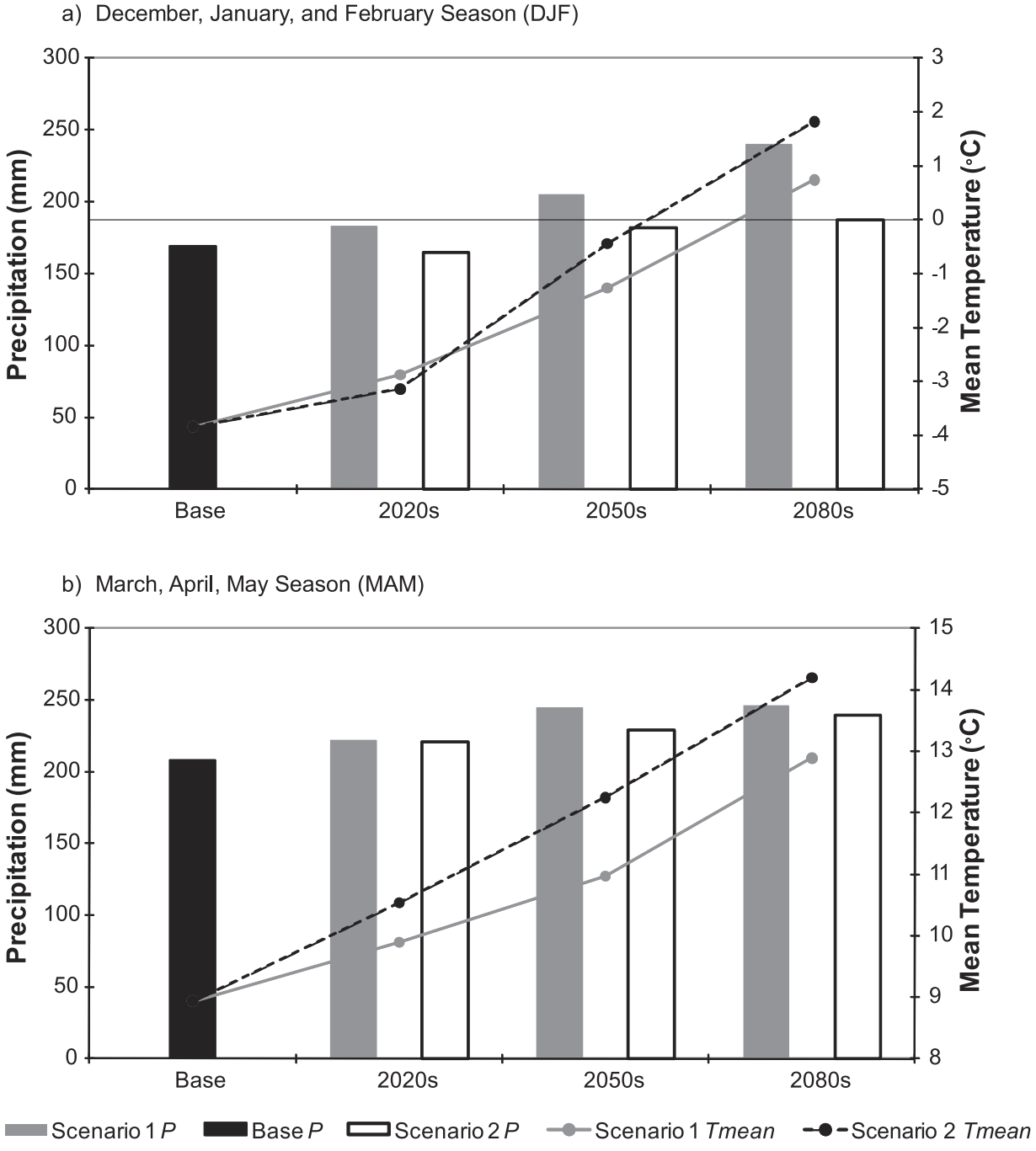

Figure 2. Changes to estimated actual seasonal mean temperature (*Tmean*; averaged from minima and maxima) and precipitation (*P*) for the St. Mary station as projected by Scenarios 1 and 2, for the three future time periods.

Weibull frequency analysis (Weibull, 1951) was used to estimate the spring runoff volume for one in ten wet and dry runoff years for historical and future scenarios. A frequency distribution plot for years 1961-1990 was developed (Figure 3). Based on Figure 3, flow volumes and percentage probability were determined for the corresponding future years (Table 3). For example, for the period 1961-1990, 1984 was a low flow year. This was year 24 within the base period. For the 2020s period, this equivalent low flow year (i.e., 9.7% probability) corresponded to the year 2033 (i.e., year 24 within the 2010-2039 period).

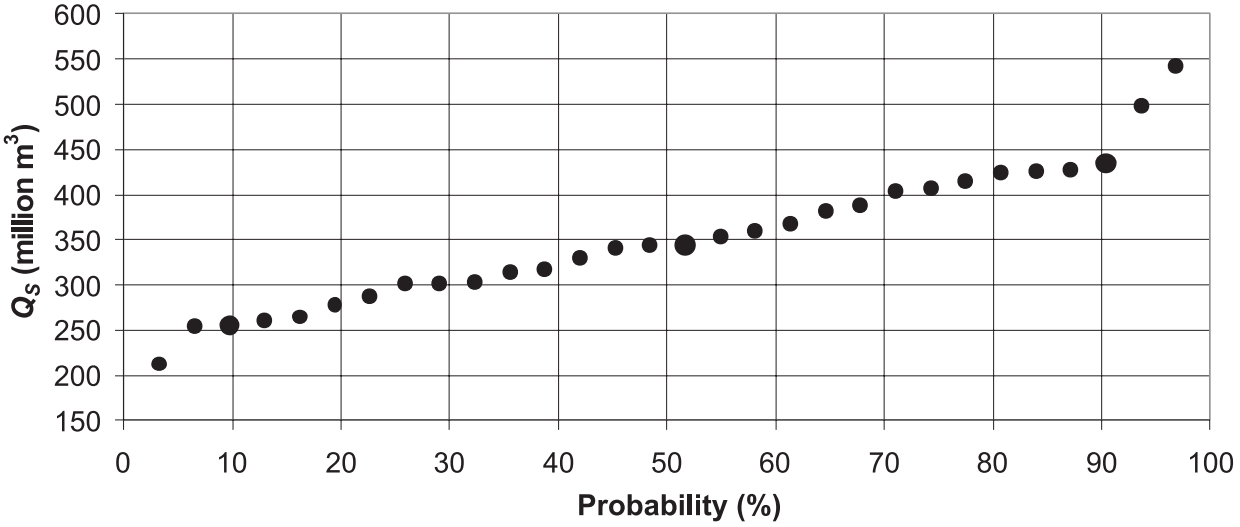

Figure 3. Weibull frequency distribution plot of the 1961-1990 modelled spring streamflow volumes. The high, median, and low Q_S years appear larger, for easy recognition.

Table 3. High, median, and low flow years used as representative years for snow hydrology comparisons. Percentage probabilities are those designated by the Weibull frequency distribution.

Modelled Q_S			Base Year	Corresponding Future Years		
Million m^3	% Prob.	Flow Type		2020s	2050s	2080s
435.4	90.3	High	1965	2014	2044	2074
345.1	51.6	Med.	1979	2028	2058	2088
255.8	9.7	Low	1984	2033	2063	2093

The corresponding years are thus representative years of high, medium, and low flow, based on the frequency distribution of the base period.

Results and Discussion

Changes in Runoff Volumes

Projected changes in snowmelt runoff (S_R), rainfall runoff (R_R) and St. Mary basin spring runoff volumes (Q_S) were generated for each scenario, using the SIMGRID Snow-Runoff model. Continuous time series of S_R, R_R, and Q_S were constructed for the 1961-2099 period (Figures 4, 5, and 6). Results for low, medium, and high flow years are presented (Table 4), to provide benchmark changes in Q_S through time.

Annual snowmelt runoff consistently declined during the historical period and for both Scenarios 1 and 2 (Figure 4), due to increases in temperature. Annual rainfall runoff was variable between scenarios 1 and 2 (Figure 5), and did not change substantially. This is explained by Figure 2, which shows that there is only a small change in precipitation during the March-April-May (MAM) season, both between scenarios and between time periods. The MAM season coincides with the rainfall runoff periods for the majority of future years. Annual streamflow, which reflects the combination of S_R and R_R variables, exhibited a modest decline with time for the historical period, a trend that extended through 2099 under both Scenario 1 and Scenario 2 (Figure 4). Despite between-scenario differences in November-June precipitation, the two Q_S projections were similar, with a trend toward slightly lower Q_S for Scenario 2 over time.

S_R and Q_S declined with time in every flow type (Table 4), under both climate scenarios. The decline in snowpack was due to warmer winter temperature, which resulted in a truncated accumulation period and enhanced mid-winter melt at lower elevations. R_R

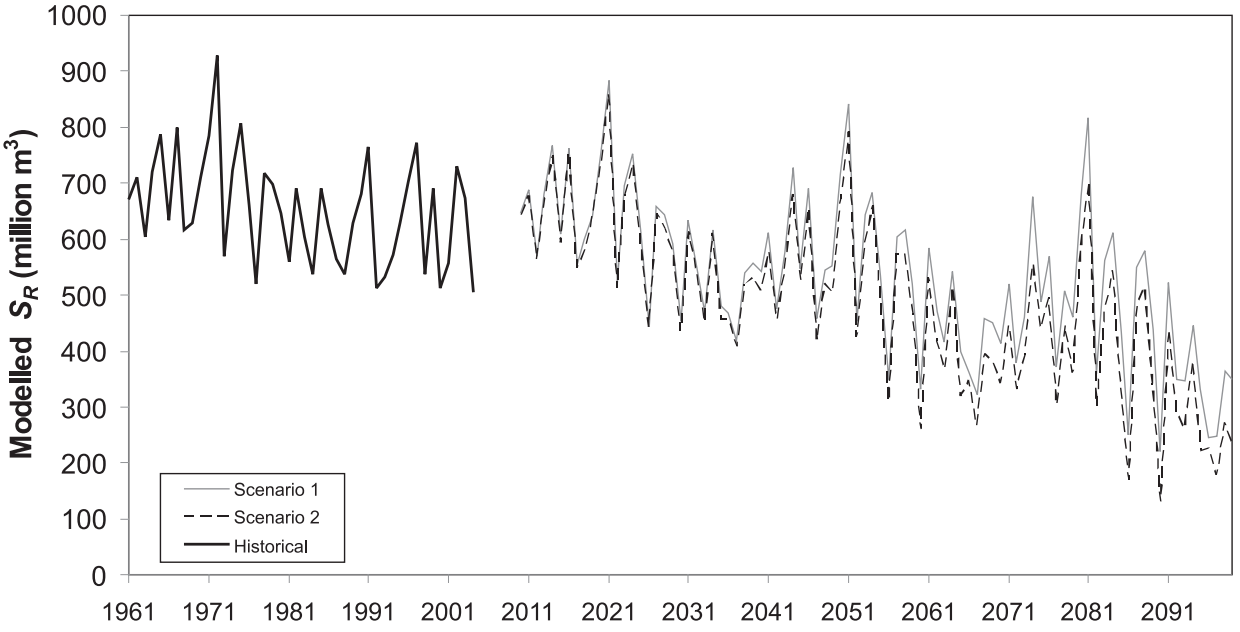

Figure 4. Modelled annual S_R for the period 1961-2099. The variability of the three future periods (i.e., 2010-2039, 2040-2069, and 2070-2099) reflects that of the base period (1961-1990). The annual time series for the three future periods serve as examples of typical years in order to illustrate possible future ranges.

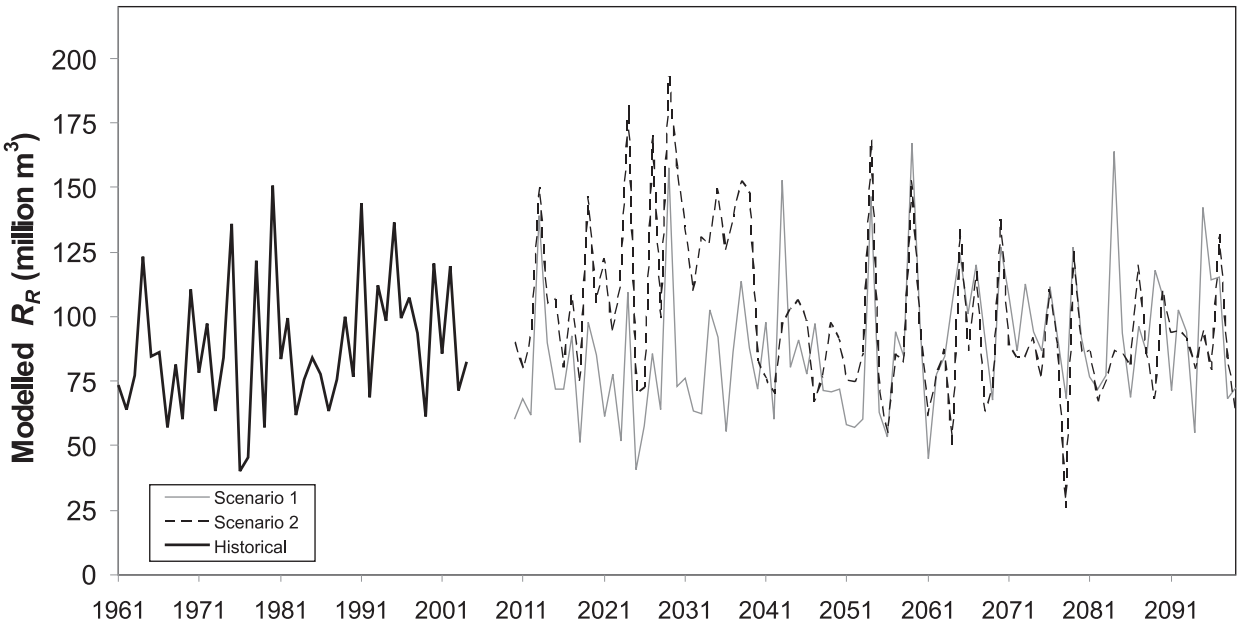

Figure 5. Modelled annual R_R for the period 1961-2099. The variability of the three future periods (i.e., 2010-2039, 2040-2069, and 2070-2099) reflects that of the base period (1961-1990). The annual time series for the three future periods serve as examples of typical years in order to illustrate possible future ranges.

increased in most cases, but the increases that occurred were small compared to the declines in S_R. The data also suggest that water supply may become restricted in low and medium flow years within a few decades, as Q_S volumes exhibited substantial declines under Scenario 1. By the 2050s, low flow Q_S was projected to decline by 29-41 percent (Table 4).

Conversion of snow to rain in the model does not appear to significantly increase R_R. Rainfall runoff occurs most routinely in the early days following

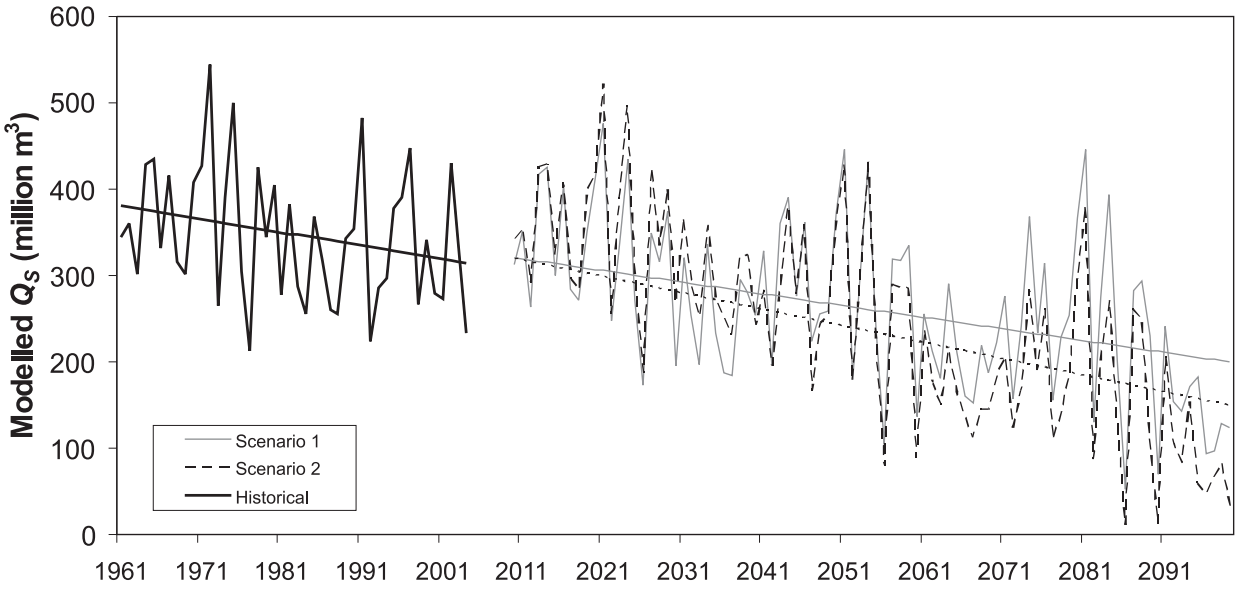

Figure 6. Modelled annual Q_S for the period 1961-2099. The variability of the three future periods (i.e., 2010-2039, 2040-2069, and 2070-2099) reflects that of the base period (1961-1990). The annual time series for the three future periods serve as examples of typical spring streamflow years in order to illustrate possible future ranges.

Table 4. Hydrologic variables under the two scenarios and three future periods, for the three flow type years. All units are in million m^3.

Period	Scenario	S_R			R_R			Q_S		
		High	Med.	Low	High	Med.	Low	High	Med.	Low
Base		787.9	696.7	538.3	84.8	56.8	75.5	435.4	345.1	255.8
2020s	1	766.4	644.2	471.1	89.9	63.9	62.1	425.8	316.3	196.5
	2	749.0	619.2	452.2	105.2	99.4	130.9	429.3	334.9	252.6
2050s	1	727.8	615.3	415.9	80.2	84.5	84.4	389.8	317.3	181.2
	2	681.7	574.2	367.6	102.9	82.4	87.5	381.1	287.1	151.4
2080s	1	676.1	579.8	345.9	94.2	85.6	94.3	368.5	294.2	143.5
	2	556.1	515.1	262.3	92.0	85.7	91.5	284.5	250.2	83.6
		Change (%)			Change (%)			Change (%)		
2020s	1	-2.7	-7.5	-12.5	6.0	12.5	-17.7	-2.2	-8.3	-23.2
	2	-4.9	-11.1	-16.0	24.1	75.0	73.4	-1.4	-3.0	-1.3
2050s	1	-7.6	-11.7	-22.7	-5.4	48.8	11.8	-10.5	-8.1	-29.2
	2	-13.5	-17.6	-31.7	21.3	45.1	15.9	-12.5	-16.8	-40.8
2080s	1	-14.2	-16.8	-35.7	11.1	50.7	24.9	-15.4	-14.7	-43.9
	2	-29.4	-26.1	-51.3	8.5	50.9	21.2	-34.7	-27.5	-67.3

snowpack disappearance when the soil is wettest from snowmelt. Evapotranspiration begins soon thereafter, and the increasing soil water deficits enhance rainfall absorption, thereby limiting R_R.

For the medium flow year of Scenario 1, modelled Q_S changed little from the 2020s to the 2050s. This can be explained by the additive nature of S_R and R_R. The DJF season climograph of Figure 2 shows that average temperatures remained below freezing, while

average precipitation increased. As a result, S_R decreased modestly from the 2020s to the 2050s (644.2 vs. 615.3 million m^3). The slightly earlier snowmelt projected by the models means that effective rainfall runoff may occur earlier in the 2050s than in the 2020s. Instead of occurring during the JJA season, when ΔP is negative (Table 3), it may occur during the MAM season, when ΔP is positive. Thus, R_R was projected to increase from 63.9 to 84.5 million m^3 between the 2020s and the 2050s. The net result of the changes in S_R and R_R is that modelled Q_S increased slightly between the 2020s and 2050s for the medium flow year. Modelled Q_S was higher for Scenario 1 than Scenario 2, except during the 2020s. This is because predicted warming rates are slightly higher for Scenario 2, while precipitation is projected to be lower during the critical November-June period. During the 2020s, Scenario 2 shows greater Q_S than Scenario 1 because of higher R_R (Table 4).

Assuming no changes would occur in temperature and precipitation frequency distributions in the future, model simulations indicated that the relative frequency of low flow years will increase in the St. Mary basin. The 1:10 year low flow Q_S is 249.5 million m^3 for the base period. The steady decline in Q_S in Table 4 and Figure 4 suggests that the historical low flow years will occur more often with time. By the 2080s, simulated Q_S volumes declined substantially, with Scenario 2 indicating mean Q_S volume lower than historical 1:10 year values.

Changes in Runoff Timing

Changes in the modelled date of snow disappearance (*Jdis*), and especially of the date of maximum snow accumulation (*Jmax*), were used as indicators of changes in runoff timing. *Jdis* refers to the complete melt out of basin snowpack, and *Jmax* is used as a proxy for the onset of spring melt. For the base period, the average date of onset of spring streamflow was April 9 (Table 5; Figure 7). Spring streamflow onset was predicted to begin about two weeks earlier in the 2020s relative to the 1961-1990 historical period. For the 2050s, average spring streamflow onset was projected to occur between March 7 (Scenario 2) and March 17 (Scenario 1). For the 2080s, simulated streamflow onset was even earlier, occurring between February 21 and March 4. Complete melt out of the basin snow occurred in June in historical times, but occurred much earlier under the future scenarios employed in this study.

The changes in timing have implications for water managers as spring flows were projected to occur much earlier, presenting challenges with later summer water supplies. As well, the snowmelt season was projected to shorten through time as the dates of maximum snow accumulation and spring streamflow onset grow closer together.

Summary

A high resolution alpine hydrometeorology model, previously calibrated for modelling spring runoff for the St. Mary River watershed (Larson *et al.*, this issue), was used to project possible impacts of climate change on spring runoff volume and timing. A series of GCM scenarios were reviewed, to estimate the trend and magnitude of possible changes in temperature and precipitation for the watershed through 2099. Two future

Table 5. Julian dates of maximum snow accumulation (*Jmax*) and snow disappearance disappearance (*Jdis*). Dates in mm/dd format are given for the three flow type years, as well as the average (Ave.) for the 30-year period.

		Jmax				*Jdis*			
Period	**Scenario**	**High**	**Med.**	**Low**	**Ave.**	**High**	**Med.**	**Low**	**Ave.**
Base		4/15	4/18	3/27	4/9	6/13	6/10	5/18	6/3
2020s	1	4/12	4/9	3/12	3/31	6/7	5/27	4/27	5/20
	2	4/8	4/3	3/5	3/26	6/3	5/21	4/20	5/15
2050s	1	3/30	3/28	2/23	3/17	5/20	5/13	4/5	5/2
	2	3/21	3/21	2/10	3/7	5/17	5/7	3/21	4/24
2080s	1	3/16	3/20	2/7	3/4	5/9	5/3	3/13	4/18
	2	3/2	3/11	1/24	2/21	4/17	4/22	2/20	3/30

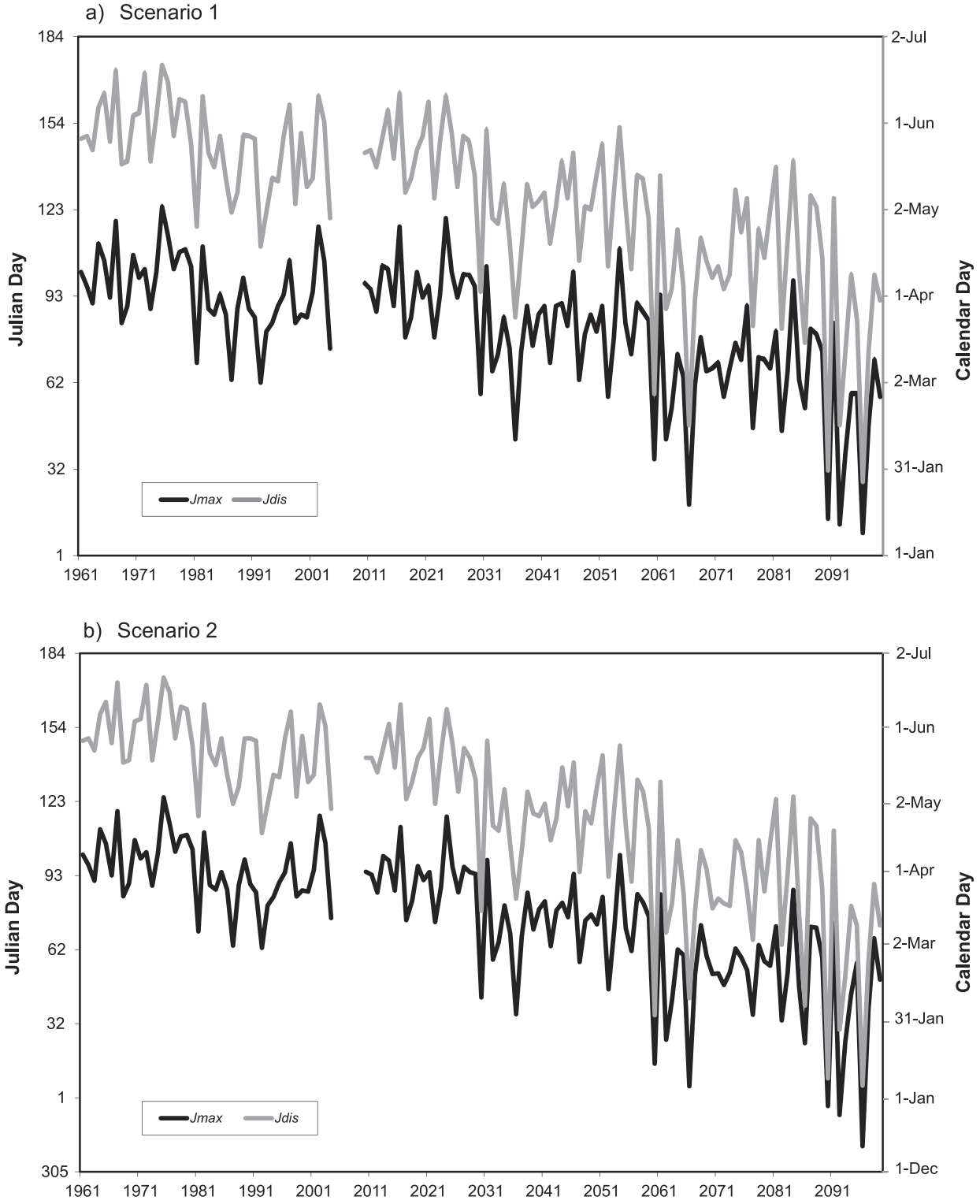

Figure 7. Modelled annual maximum snow accumulation (*Jmax*) and snow disappearance (*Jdis*) dates for the period 1961-2099. The variability of the three future periods (i.e., 2010-2039, 2040-2069, and 2070-2099) reflects that of the base period (1961-1990). The annual time series for the three future periods serve as examples of typical spring streamflow years in order to illustrate possible future ranges.

scenarios were selected that envelop the upper and lower range of possible precipitation change that will likely occur within the watershed as global warming progresses through 2099. The results should be interpreted with an understanding that there is a degree of uncertainty in GCM model projections, and that it was assumed that the relationships for which the SIMGRID Snow-Runoff model were validated for the historical period (Larson *et al.*, this issue), will remain valid in the future.

Both scenarios forecast substantial warming, with only small increases in precipitation during winter and spring. Under the adopted scenarios, spring runoff declined substantially during the 90-year simulation period. While the predicted impacts of climate warming on streamflow were modest for the 2020s, more substantial and progressive declines were predicted for the 2050s and 2080s.

The main factors predicted to reduce spring streamflow include higher rain:snow ratios and higher snowmelt frequency in winter, due to higher temperatures. This is expected to produce a decrease in basin snow water equivalent in spring, earlier spring streamflow onset and lower spring streamflow volume, despite small increases in projected precipitation. These changes would likely result in severe water shortages during drought years. Earlier snowmelt onset will present challenges for water storage facilities, even during average years. The changing winter period will also have implications for winter recreation and a range of ecosystem dynamics such as land cover relationships with fire season length and intensity and instream flows.

Acknowledgements

This work was funded by the Alberta Ingenuity Centre for Water Research under Theme 1 (Watersheds). We appreciate the many comments received from anonymous reviewers, which helped to improve the manuscript. The authors also thank Katherine Forbes and Ryan MacDonald for their insightful discussions and help in developing portions of the methodology.

References

Alberta Agriculture, Food & Rural Development (AAFRD). 2000. *Irrigation in Alberta, Part 2*, Alberta Agriculture, Food & Rural Development, Lethbridge, AB.

Barnett, T. P., J. C. Adam, and D. P. Lettenmaier. 2005. Potential impacts of a warming climate on water availability in snow-dominated regions. *Nature* 438(17): 1-7.

Barrow, E., and G. Yu. 2005. *Climate Scenarios for Alberta*, 73 pp, Alberta Environment and PARC (Prairie Adaptation Research Collaborative), Regina, Saskatchewan.

Betts, R. A. 2004. Global vegetation and climate: Self -beneficial effects, climate forcings and climate feedbacks. *Journal de Physique* IV(121): 3-60.

Bond, N. A., J. E. Overland, M. Spillane, and P. Stabeno. 2003. Recent shifts in the state of the North Pacific. *Geophysical Research Letters* 30(23): 2183. doi:10.1029/2003GL018597.

Bonsal, B., T. D. Prowse, and A. Pietroniro. 2003. An assessment of global climate model-simulated climate for the western cordillera of Canada (1961-90). *Hydrological Processes* 17: 3703-3716.

Brown, R. D., and R. O. Braaten. 1998. Spatial and temporal variability of Canadian Monthly snow depths, 1946-1995. *Atmosphere-Ocean* 36(1): 37-54.

Byrne, J., S. Kienzle, G. Duke, V. Gannon, B. Selinger, and J. Thomas. 2006. Current and future water issues in the Oldman River Basin, Alberta, Canada. *Water Science and Technology* 53(10): 327-334.

Carter, T., M. Hulme, and M. Lal. 1999. *Guidelines on the Use of Scenario Data for Climate Impact and Adaptation Assessment.* Prepared by the Intergovernmental Panel on Climate Change, Task Group on Scenarios for Climate Impact Assessment [IPCC-TGCIA]. Intergovernmental Panel on Climate Change, Geneva, Switzerland. 69 pp.

Christensen, J. H., B. Hewitson, A. Busuioc, A. Chen, X. Gao, I. Held, R. Jones, R. K. Kolli, W. –T. Kwon, R. Laprise, V. M. Rueda, L. Mearns, C. G. Menéndez, J. Räisänen, A. Rinke, A. Sarr, and P. Whetton. 2007. *Regional Climate Projections*. Intergovernmental Panel on Climate Change, Cambridge, UK, and New York, USA.

Cubasch, U., G. A. Meehl, and G. J. Boer. 2001. Projections of future climate change, in *Climate Change 2001: The Scientific Basis. Contribution of Working Group I to the Third Assessment Report of the Intergovernmental Panel on Climate Change*, edited by J. T. e. a. Houghton, pp. 525-582, Cambridge University Press.

Diffenbaugh, N.S., J.S. Pal, R. J. Trapp., and F. Giorgi. 2005. Fine-scale processes regulate the response of extreme events to global climate change. *Proceedings of the National Academy of Sciences of the United States of America.* 102(44): 15774-15778.

Field, C. B., L. D. Mortsch, M. Brklacich, D. L. Forbes, P. Kovacs, J. A. Patz, S. W. Running, and M. J. Scott. 2007. *North America*, 617-652 pp, Cambridge University Press, Cambridge, UK.

Groisman, P. Y., T. R. Karl, and R. W. Knight. 1994. Changes of snow cover, temperature, and radiative heat balance over the Northern Hemisphere. *Journal of Climate* 7(11): 1633-1656.

Halliday, R., and G. Faveri. 2007. The St. Mary and Milk Rivers: The 1921 Order revisited. *Canadian Water Resources Journal* 32(1): 75-92.

Hamlet, A. F., P. W. Mote, M. P. Clark, and D. P. Lettenmaier. 2005. Effects of temperature and precipitation variability on snowpack trends in the Western United States. *Journal of Climate* 18: 4545-4561.

Hauer, F. R., J. S. Baron, D. H. Campbell, K. D. Fausch, S. W. Hostetler, G. H. Leavesley, P. R. Leavitt, D. M. Mcknight, and J. A. Stanford. 1997. Assessment of climate change and freshwater ecosystems of the Rocky Mountains, USA and Canada. *Hydrological Processes* 11: 903-924.

Hungerford, R. D., R. R. Nemani, S. W. Running, and J. C. Coughlan. 1989. *MTCLIM: Mountain Microclimate Simulation Model. Research Paper INT-414*, 52 pp, U.S. Department of Agriculture, Forest Service, Intermountain Research Station, Ogden, UT.

Huntington, T. G. 2006. Evidence for intensification of the global water cycle: Review and synthesis. *Journal of Hydrology*. 319(1): 83-95

Karl, T. R., P. Y. Groisman, R. W. Knight, and R. R. Heim. 1993. Recent variations of snow cover and snowfall in North America and their relation to precipitation and temperature variations. *Journal of Climate* 6: 1327-1344.

Knowles, N., M. D. Dettinger, and D. R. Cayan. 2006. Trends in snowfall versus rainfall in the Western United States. *Journal of Climate* 19: 4545-4559.

Langen, N., M. D. Dettinger, and D. R. Cayan. 2007. Cloud variability, radiative forcing and meridional temperature gradients in a general circulation model *Tellus Series A - Dynamic Meteorology and Oceanography* 59(5): 641-649.

Larson, R. P., J. M. Byrne, D. L. Johnson, M. G. Letts and S. W. Kienzle. this issue. Modelling climate change impacts on spring runoff for the Rocky Mountains of Montana and Alberta I: Model development, calibration and historical analysis. *Canadian Water Resources Journal*. 36(1):17-34:

Lapp, S., J. M. Byrne, S. W. Kienzle, and I. Townshend. 2002. Linking global circulation model synoptics and precipitation for western North America. *International Journal of Climatology* 22: 1807-1817.

Lapp, S., J. M. Byrne, S. W. Kienzle, and I. Townshend. 2005. Climate warming impacts on snowpack accumulation in an alpine watershed: A GIS based modeling approach. *International Journal of Climatology* 25(4): 521-526.

Lettenmaier, D. P., E. F. Wood, and J. R. Wallis. 1994. Hydro-climatological trends in the continental United States, 1948-88. *Journal of Climate* 7: 586-607.

Leung, L. R., and M. S. Wigmosta. 1999. Potential climate change impacts on mountain watersheds in the Pacific Northwest. *Journal of the American Water Resources Association* 35: 1463-1471.

Leung, L. R., A. F. Hamlet, D. P. Lettenmaier, and A. Kumar. 1999. Simulations of the ENSO hydroclimate signals in the Pacific Northwest Columbia River Basin. *Bulletin of the American Meteorological Society* 80(11): 2313-2329.

Leung, L. R., Y. Qian, X. Bian, W. M. Washington, J. Han, and J. O. Roads. 2004. Mid-century ensemble regional climate change scenarios for the western United States. *Climatic Change* 62: 75-113.

Loukas, A., L. Vasiliades, and N. R. Dalezios. 2002. Potential climate change impacts on flood producing mechanisms in southern British Columbia, Canada using the CGCMA1 simulation results. *Journal of Hydrology* 259(1-4): 163-188.

Loukas, A., L. Vasiliades, and N. R. Dalezios. 2004. Climate change implications on flood response of a mountainous watershed. *Water, Air and Soil Pollution: Focus* 4(4-5): 331-347.

McCabe, G. J., and D. M. Wolock. 1999. General-Circulation-Model simulations of future snowpack in the Western United States. *Journal of the American Water Resources Association* 35(6): 1473-1483.

Merritt, W. S., Y. Alila, M. Barton, B. Taylor, S. Cohen, and D. Neilsen. 2006. Hydrologic response to scenarios of climate change in sub watersheds of the Okanagan basin, British Columbia. *Journal of Hydrology* 326(1-4): 79-107.

Morrison, J., M. C. Quick, and M. G. G. Foreman. 2002. Climate change in the Fraser River watershed: flow and temperature projections. *Journal of Hydrology* 263(1-4): 230-244.

Mote, P. W. 2003. Trends in snow water equivalent in the Pacific Northwest and their climatic causes. *Geophysical Research Letters* 30(12): 1-4.

Mote, P. W., A. F. Hamlet, M. P. Clark, and D. P. Lettenmaier. 2005. Declining mountain snowpack in Western North America. *American Meteorological Society* 86(1): 39-49.

Nakićenović, N., *et al.* 2000. *IPCC Special Report on Emissions Scenarios*, 599 pp. Cambridge University Press, Cambridge, UK and New York, USA.

Nash, L. L., and P. H. Gleick. 1991. Sensitivity of streamflow in the Colorado Basin to climatic changes. *Journal of Hydrology* 125(3-4): 221-241.

Newman, M., G. P. Compo, and M. A. Alexander. 2003. ENSO-forced variability of the Pacific Decadal Oscillation. *Journal of Climate* 16(23): 3853-3857.

Overland, J. E., and M. Wang. 2007. Future climate of the North Pacific Ocean. *Eos* 88(16): 178-182.

Pacific Climate Impacts Consortium (PCIC). 2007. *Scenario Access Interface*. http://www.pacificclimate.org/impacts/ (accessed April 2007.)

Qu, X., and A. Hall. 2007. What controls the strength of the snow- albedo feedback? *Journal of Climate* 20(15): 3971-3981.

Rood, S. B., J. M. Mahoney, D. E. Reid, and L. Zilm. 1995. Instream flows and the decline of riparian cottonwoods along the St. Mary River, Alberta. *Canadian Journal of Botany* 73: 1250-1260.

Rood, S. B., G. M. Samuelson, J. K. Weber, and K. A. Wywrot. 2005a. Twentieth-century decline in streamflows from the hydrographic apex of North America. *Journal of Hydrology* 306(1-4): 215-233.

Rood, S. B., G. M. Samuelson, J. H. Braatne, C. R. Gourley, F. M. R. Hughes, and J. M. Mahoney. 2005b. Managing river flows to restore floodplain forests. *Frontiers in Ecology* 3(4): 193-201.

Rood, S. B., J. Pan, K. M. Gill, C. G. Franks, G. M. Samuelson, and A. Shepherd. 2008. Declining summer flows of Rocky Mountain rivers: Changing seasonal hydrology and probably impacts on floodplain forests. *Journal of Hydrology* 349(3-4): 397-410.

Sanderson, B. M., G. M. Samuelson, J. K. Weber, and K. A. Wywrot. 2005. Twentieth- century decline in streamflows from the hydrographic apex of North America. *Journal of Hydrology* 306(1-4): 215-233.

Schindler, D. W., and W. F. Donahue. 2006. An impending water crisis in Canada's western prairie provinces. *Proceedings of the National Academy of Science USAS* 103(19): 7210-7216.

Selkowitz, D. J., D. B. Fagre, and B. A. Reardon. 2002. Interannual variations in snowpack in the Crown of the Continent Ecosystem. *Hydrological Processes* 16: 3651-3665.

Shabbar, A., and B. Bonsal. 2003. An assessmnet of changes in winter cold and warm spells over Canada. *Natural Hazards* 29(2): 173-188.

Shepperd, A. 1996. Modelling Hydrometeorology in the Upper Oldman River Basin. M.Sc. Thesis, 178 pp, University of Lethbridge, Lethbridge.

Stewart, I. T., D. R. Cayan, and M. D. Dettinger. 2004. Changes in snowmelt runoff timing in Western North America under a 'business as usual' climate change scenario. *Climatic Change* 62: 217-232.

Stewart, I. T., D. R. Cayan, and M. D. Dettinger. 2005. Changes toward earlier streamflow timing across Western North America. J*ournal of Climate* 18: 1136-1115.

Vincent, L. A., X. Zhang, and W. D. Hogg. 1999. Maximum and minimum temperature trends in Canada for 1895-1995 and 1945-1995, paper presented at 10th Symposium on Global Change Studies, American Meteorological Society, Dallas, TX.

Von Storch, H., E. Zorita, and U. Cubasch. 1993. Downscaling of global climate change estimates to regional scales: an application to Iberian rainfall in wintertime. *American Meteorological Society* 6: 1161-1171.

Weibull, W. 1951. A statistical distribution function of wide applicability. *Journal of Applied Mechanics* 18: 293-297.

Whitfield, P. H., C. J. Reynolds, and A. Cannon. 2002. Modelling streamflow in present and future climates: example from the Georgia basin, British Columbia. *Canadian Water Resources Journal* 27(4): 427-456.

List of Acronyms/Terms/Variables

DJF	December-January-February season
GCM	Global Circulation Model
JJA	June-July-August season
MAM	March-April-May season
MLR	Multiple Linear Regression
MTCLIM	Mountain Microclimate Model
SIMGRID	Simulated Grid microclimate model
SNOPAC+ROS	Snowpack accumulation/ablation program
SON	September-October-November season
SWE	Snow water equivalent
TC	Terrain Category
WNA	Western North America
Historical Period	1961-2004
Base Period	1961-1990
2020s	2010-2039
2050s	2040-2069
2080s	2070-2099
Jdis	Julian date of snowpack depletion
Jmax	Julian date of maximum snow accumulation
P	Precipitation
Q_S	Spring runoff volume
R_R	Rainfall runoff volume
S_R	Snowmelt runoff volume
Tmax	Maximum temperature
Tmean	Mean temperature
Tmin	Minimum temperature